Top Catal (2011) 54:135–145
DOI 10.1007/s11244-011-9652-7

ORIGINAL PAPER

Influence of Drying Conditions on Amine-Functionalized SBA-15 as Adsorbent of CO_2

G. Calleja · R. Sanz · A. Arencibia · E. S. Sanz-Pérez

Published online: 27 January 2011

Abstract Adsorption of pure CO_2 on amine-functionalized SBA-15 mesoporous silica materials has been studied. Adsorbent materials were prepared by grafting the silica surface with aminopropyl (AP), ethylene-diamine (ED) and diethylene-triamine (DT) organosilane molecules. Materials so obtained were dried under air atmosphere at 110 °C and at room temperature. CO_2 adsorption isotherms were carried out at 45 °C, showing that grafted materials are very efficient for CO_2 removal at atmospheric pressure when samples are dried at 20 ° C. However, when the drying step is carried out at 110 °C in air, CO_2 adsorption capacity is low. DRIFTS analysis has shown that amino groups can undergo oxidation to oxime or imine species during drying. Adsorption capacity of the materials was found to be unchanged after some consecutive adsorption–desorption cycles, being the regeneration step performed at 110 °C under vacuum.

Keywords Mesoporous silica · SBA-15 · CO_2 adsorption · Amine functionalization · Amine degradation · Carbon capture sequestration (CCS)

G. Calleja (✉) · R. Sanz · A. Arencibia · E. S. Sanz-Pérez
Department of Chemical and Energy Technology, ESCET, Universidad Rey Juan Carlos, C/Tulipán s/n, 28933 Móstoles, Madrid, Spain
e-mail: guillermo.calleja@urjc.es

R. Sanz
e-mail: raul.sanz@urjc.es

A. Arencibia
e-mail: amaya.arencibia@urjc.es

E. S. Sanz-Pérez
e-mail: eloy.sanz@urjc.es

1 Introduction

The CO_2 increasing emissions to the atmosphere are producing a growing concern because their effect on global environmental warming. As a consequence, carbon capture and sequestration (CCS) has become a crucial issue [1–5] to reduce these emissions and contribute to a cleaner use of fossil fuels.

Present available techniques for CO_2 capture are based on large scale absorption processes that involve carbon dioxide reaction with liquid amines, like monoethanolamine (MEA), diethanolamine (DEA) and methyl-diethanolamine (MDEA) [6–8]. However, these processes have major disadvantages that limit their efficiency, basically related to the high energy consumption during absorbent regeneration, solvent deterioration, and evaporation and corrosion produced by the liquid solutions [9, 10]. Consequently, a number of alternative capture techniques are being developed in the last years, like membrane-based separation processes, cryogenic technologies or gas phase adsorption on efficient porous materials [11].

Well-known adsorbents such as activated carbons and zeolites can achieve high adsorption capacities at high pressures and low temperatures, but pressurizing costs are very high. An alternative is to develop new selective adsorbent materials that reach high CO_2 adsorption capacities at atmospheric pressure and at a temperature higher than 45 °C. The functionalization of porous materials with organic molecules containing amino groups is aiming to a double objective: first, amino-functionalized materials can be very selective, providing higher CO_2 adsorption capacities at lower pressures [12], and second, grafted amino group-containing molecules on the adsorbent surface of solid materials are less toxic and corrosive compared to the liquid phase amine molecules, and can be

more easily regenerated. Amine basic functionalities chemically react with CO_2 acidic molecules, producing stable carbamate species [13]. As a result, chemisorption processes lead to higher CO_2 adsorption capacities at low pressure, minimizing toxicity and corrosiveness.

Mesostructured solids present a narrow pore size distribution that can usually be tuned during the synthesis process. Their high surface area and pore volume values favor the anchorage of organic groups and also a rapid diffusion of gas molecules through the inner pores [14]. For this reason, these materials are very convenient for being functionalized with organic molecules for specific purposes, like CO_2 capture. In this work, SBA-15 has been selected with preference to other mesostructured materials due to its relatively wide channel mesoporous structure with high values of surface area and pore volume, and also to its high thermal and hydrothermal stability, related to the large pore wall thickness of the resulting structure [15].

Organic functionalization processes of solid surfaces for CO_2 capture can be done by impregnation, co-condensation and grafting. Impregnation with organic molecules over several supports has been extensively studied. Among other aminated molecules, poly-ethyleneimine (PEI) [12, 16–22] and tetraethylene-pentamine (TEPA) [21–28] are presented as convenient compounds since both of them contain a large number of amino groups in the molecule. In particular, silica SBA-15 impregnated with PEI shows adsorption capacity values at 45 °C up to 88 mg CO_2/g at a pressure of 1 bar of pure CO_2 [12].

Compared to impregnation, co-condensation and grafting techniques provide covalent bonds between functionalizing agents and surface sites of solid supports. In the case of SBA-15, which is synthesized in acidic medium, co-condensation of amine-containing organosilane molecules produce materials with a substantial part of the functional groups incorporated to the support walls [29], which are in practice difficut to reach by the adsorbates [30].

Grafting techniques, however, yield functionalized materials with higher amine content, being practically all of the loaded amino groups accessible to the adsorbate molecules. Hence, alcoxysilanes containing amino groups have been early used for functionalizing silica materials [31] in order to capture CO_2 [32–36]. These organosilane molecules can contain one [32, 33], two [34] and three [35, 36] amino groups and can be anchored to silica supports through the silanol groups of the silica surface. The resulting materials are considered as potential adsorbents for efficient CO_2 capture. Amino-propyl (AP (N)), ethylene-diamine (ED (NN)) and diethylene-triamine (DT (NNN)) molecules are some of the functionalizing organosilane compounds considered for this purpose due to their relative high nitrogen content and appropriate molecular structure and size.

In this paper the functionalization of SBA-15 mesostructured silica by grafting with different amounts of the three amine molecules above mentioned, AP (N), ED (NN) and DT (NNN) is reported. The drying step conditions after functionalization with the amine molecules and its effect on the CO_2 adsorption capacity of the resulting material have been thoroughly studied. Several drying temperature and drying time values have been considered to test the amine-group stability. Finally, successive adsorption–desorption cycles have been performed, carrying out the regeneration step at 110 °C under vacuum.

2 Experimental Section

2.1 Preparation of Pure SBA-15

SBA-15 mesostructured silica was synthesized following the original procedure described by Zhao et al. [15]. Pluronic P123 ($PEO_{20}PPO_{70}PEO_{20}$, Mn ~ 5800, Sigma-Aldrich) was used as a structure directing agent and TEOS (tetraethyl orthosilicate, 98 %, Sigma-Aldrich) as a silica source. A large scale synthesis was performed obtaining up to 40 g of SBA-15, following a procedure previously reported by our group [12]. In summary, the desired amount of Pluronic P123 was dissolved in a 1.9 M hydrochloric acid solution and the mixture stirred until complete dissolution. Then, TEOS was added to the acidic medium keeping the mixture at 40 °C for 20 h. After that, an ageing step at 110 °C for 24 h was carried out to complete the formation of the SBA-15 siliceous structure. The obtained solid was then filtered and calcined in air at 550 °C to remove the surfactant from the porous structure.

2.2 Functionalization of SBA-15 with Organosilane Molecules Containing Amino Groups

Figure 1a shows the three organosilane molecules selected form Sigma–Aldrich, having the following structure: (i) Aminopropyl, with one primary amino group and abbreviated as AP (N), (ii) ethylene-diamine, with two amino groups (one primary and one secondary amine) abbreviated as (ED (NN)), and (iii) diethylene-triamine, with one primary amino group and two secondary groups, abbreviated as (DT (NNN)). Figure 1b shows, as an example, the functionalization reaction scheme with SBA-15, performed via post-synthesis grafting with the DT (NNN) molecule. In this reaction, each metoxy group (−OMe) of the organosilane molecule reacts with one silanol group (−SiOH) of the SBA-15 surface. As a result, a covalent bond is formed between the organic molecule and the silica support, allowing the anchorage of the amino groups to the silica surface.

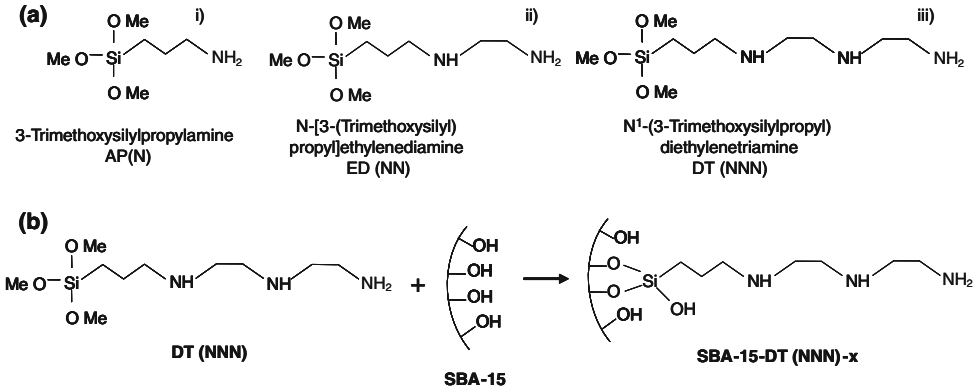

Fig. 1 Schematic representation of AP (N), ED (NN) and DT(NNN) molecules (**a**) and functionalization of SBA-15 with DT (NNN) by grafting (**b**)

The experimental procedure for functionalization was as follows: First, 1 g of SBA-15 was dispersed in 250 mL of toluene and stirred for 10 min. Then, the desired amount of functionalizing agent was added to the mixture and keeping the system under reflux for 24 h. After that, the solid was filtered and washed with 200 mL of toluene in order to remove the excess of organosilane. Synthesized samples were named SBA-15-AP (N)-*x*, SBA-15-ED (NN)-*x* and SBA-15-DT (NNN)-*x*, where *x* represents the hypothetical number of existing silanol groups per square nanometer of SBA-15 silica surface. According to van der Voort et al. [37], a reasonable value of this number was estimated to be 1.7 SiOH/nm^2 when calcining silica at 550 °C. A similar situation was assumed for SBA-15 and a 1:1 reaction was supposed to take place between surface silanol groups and organosilane molecules. Thus, taking into account the surface area value obtained for pure silica SBA-15, the amount of organic amine to be loaded to the silica was calculated.

According to this procedure, the following materials were prepared: SBA-15-AP (N)-2, SBA-15-ED (NN)-2 and SBA-15-DT (NNN)-2, corresponding to silanol ratios of 2 SiOH/nm^2 (very close to the mentioned stoichiometric value for silica, 1.7 SiOH/nm^2), as well as SBA-15-AP (6), SBA-15-ED (6) and SBA-15-DT (6), corresponding to silanol ratios of 6 SiOH/nm^2, that is three times higher to provide an excess of organic compound.

Two drying conditions were studied in order to evaluate the effect of drying temperature and time on the CO_2 adsorption properties of the materials: a) drying at room temperature in air for one day (20 °C, 24 h) and b) drying at 110 °C in air for various times (6, 24 and 72 h).

2.3 Characterization Techniques

Low angle X-Ray diffraction measurements of pure SBA-15 silica and functionalized samples were performed with a powder diffractometer PHILIPS X-PERT MPD with a CuKα monochromatic radiation.

Nitrogen adsorption–desorption isotherms at 77 K were obtained in a MICROMERITICS TRISTAR-3000 sorptometer. SBA-15 material was outgassed at 200 °C in N_2 flow, while organic-containing samples were outgassed at 150 °C in N_2 flow. Surface area values were calculated with B.E.T. equation, pore size distributions were determined from the adsorption branch by using the B.J.H. model with cylindrical pore geometry and total pore volumes were obtained at $P/P_0 \geq 0.97$.

Elemental analysis of carbon, nitrogen and hydrogen was carried out in an ELEMENTAL analyzer Vario EL III equipped with a thermal conductivity detector.

In situ diffuse reflectance infrared spectra (DRIFTS) were collected with a FTIR Mattson Infinity Series Spectrometer with a DTGS detector. The samples were placed in a commercial Low Temperature Reaction Chamber CHC-CHA working at high vacuum and coupled to a diffuse reflectance accessory (Praying Mantis).

2.4 CO_2 Adsorption Measurements

Pure CO_2 adsorption isotherms were measured with a volumetric analyzer (Scientific Instruments HPVA-100, VTI) at 45 °C in a pressure range 1–6 bar. The outgassing step was carried out at 110 °C for 2 h under 10^{-3} mbar vacuum prior to the measurements. A double equilibrium criteria was used: a pressure drop lower than 0.2 mbar in 3 min or a maximum equilibration time of 60 min.

3 Results and Discussion

3.1 Characterization of the Adsorbent Materials

Figure 2 shows low angle XRD diffractograms obtained for pure SBA-15 and also for amine-functionalized SBA-15 materials with 2 or 6 SiOH/nm^2 dried at room temperature. As observed, mesostructured SBA-15 silica has a well defined hexagonal porous structure [15], according to

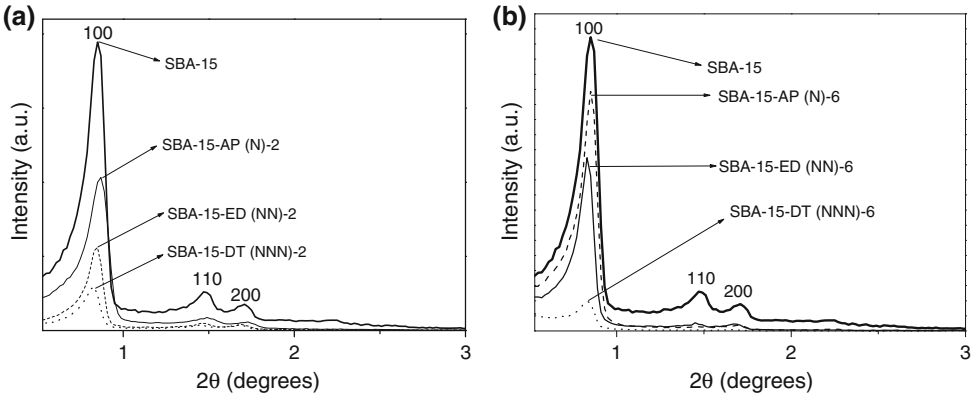

Fig. 2 XRD patterns for amine-functionalized SBA-15 materials with: (**a**) 2 SiOH/nm^2 and (**b**) 6 SiOH/nm^2

the intense main signal corresponding to the (1 0 0) plane family and to the two small diffraction peaks at higher angles. Functionalized samples show patterns having the same diffraction peaks, with intensities that gradually diminish as the size of the grafted organic chain is increased. This drop is almost certainly due to the partial pore filling with organic chains, giving as a result a material through which X-Ray constructive interferences are attenuated. However, SBA-15 structure is preserved even after functionalization up to 6 SiOH/nm^2.

N_2 adsorption–desorption isotherms and pore size distributions of pure SBA-15 functionalized samples dried at room temperature are shown in Fig. 3. SBA-15 silica presents the classic type IV isotherm according to IUPAC, co-existing micro and mesoporous in its structure.

Textural properties and nitrogen content of pure and functionalized SBA-15 samples are summarized in Table 1. SBA-15 silica has typical values of surface area (692 m^2/g), pore volume (1.03 cm^3/g) and pore diameter (9.0 nm). Functionalized samples exhibit lower surface area values, as expected, due to partial pore filling with the amine molecules resulting from grafting. As shown in Fig. 3a, b, when the organosilane compounds are added at ratios of 2 or 6 SiOH/nm^2, the resulting isotherms of the obtained materials show a significant reduction in nitrogen adsorption. These changes are in both cases more pronounced as the length of the amine molecule loaded is increased. Accordingly, surface area and pore volume values decrease in the order AP (N) > ED (NN) > DT (NNN). Pore size distribution, plotted in Fig. 3, is also changed after functionalization. A decrease in the intensity of the peaks is observed, more evident in general for a higher nitrogen content and a longer chain length of the functionalizing amine molecule.

Table 1 also shows the nitrogen content of grafted samples (measured by elemental analysis), which is clearly influenced by the type of organosilane compound used for grafting and the amount loaded. It is observed that the resulting nitrogen content of the sample increases when the organic chain contains more amino groups (DT (NNN) > ED (NN) > AP (N)) or when more molecule chains are incorporated into the support (6 OH/nm^2 > 2 OH/nm^2), as expected, reaching values up to 7.3%.

3.2 CO_2 Adsorption Capacity

Pure CO_2 adsorption–desorption isotherms at 45 °C corresponding to SBA-15 functionalized samples dried at room temperature are shown in Fig. 4. The amount of CO_2 adsorbed is measured in mg of CO_2 per gram of adsorbent and plotted against equilibrium pressure. CO_2 adsorbed concentrations at 1 and 5.5 bar are also shown in Table 2.

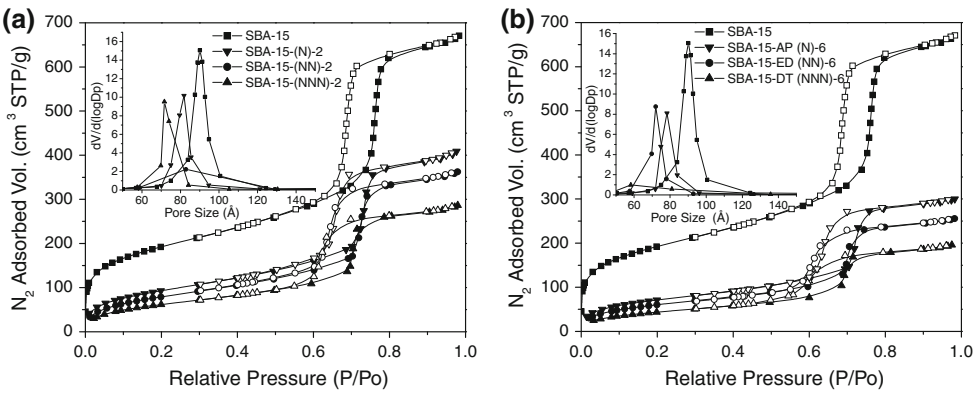

Fig. 3 Nitrogen adsorption–desorption isotherms at 77 K for SBA-15 and functionalized samples with: (**a**) 2 SiOH/nm^2 and (**b**) 6 SiOH/nm^2

Table 1 Textural properties of SBA-15 functionalized samples with 2 and 6 SiOH/nm^2

Adsorbent	S_{BET} (m^2/g)	D_{PORE} (nm)	V_{PORE} (cm^3/g)	wt % N
SBA-15	692	9.0	1.03	–
SBA-15-AP (N)-2	347	8.2	0.62	2.6
SBA-15-ED (NN)-2	299	8.3	0.55	4.8
SBA-15-DT (NNN)-2	235	7.2	0.44	6.3
SBA-15-AP (N)-6	266	7.8	0.46	3.7
SBA-15-ED (NN)-6	228	7.2	0.39	5.7
SBA-15-DT (NNN)-6	166	5.8	0.30	7.3

Considering the isotherm curves of Fig. 4, two different trends are observed. Firstly, SBA-15 pure silica material presents low adsorption capacities at low pressures and a significant adsorption increase as CO_2 pressure rises. This pressure-dependent isotherm is characteristic of physisorption processes, as occur in many classical adsorbents such as activated carbons [38] and zeolites [39].

Amino functionalized materials, however, show a much higher CO_2 adsorption capacity at atmospheric pressure than raw SBA-15, and a less pronounced adsorption increase with pressure. The amount of adsorbed CO_2 is also favored when increasing the nitrogen content of the molecule (DT (NNN) > ED (NN) > AP (N)). Thus, when functionalizing SBA-15 with DT (NNN) amine for 6 SiOH/nm^2, the adsorption capacity achieved at 1 bar (76.8 mg CO_2/g ads, Table 2) is even higher than the capacity attained by pure SBA-15 at 5.5 bar. This high efficiency in adsorption at low pressure, as well as the partial irreversibility observed in the isotherms for the functionalized materials, is related to a chemisorption mechanism, as it has been previously explained for similar adsorbents [12]. From this point of view, the amino groups and therefore the presence of a larger amount of N atoms in the functionalizing molecule is clearly determining the extent of CO_2 adsorption. This effect is dominant and compensates the decrease of pore volume resulting from a larger functionalizating molecule. It has to be considered, anyway, that the pore volume is in all cases rather large, so that diffusional restrictions are not really expected.

The fact that amine functionalized materials obtained by grafting present a high CO_2 adsorption capacity even at very low pressures can have an important application, since industrial CO_2-containing combustion gases in typical coal power stations are discharged, after desulphurization, at 40–50 °C and atmospheric pressure. So, a high adsorption capacity at low pressure resulting from chemisorption would avoid expensive pressurizing steps, necessary when using other materials where physisorption controls the adsorption process.

Table 2 also lists CO_2 molar adsorption capacity values referred to the nitrogen content of the material. A constant value of 0.3 mol of CO_2 per mole of nitrogen is obtained for an organosilane loading of 2 SiOH/nm^2 regardless of the type of amine molecule used for grafting. Values in the range 0.34–0.42 are obtained when the loading is higher (6 SiOH/nm^2), but this ratio decreases when increasing the chain length.

Further comments for each individual amine molecule should be mentioned. In the case of the aminopropyl (AP (N)) molecule, with only one amino group in its chain, an increase in the relative adsorption capacity from 0.32 to 0.42 mol of CO_2 per mole of nitrogen is observed when increasing amine loading, probably due to the proximity of AP anchored molecules which favors CO_2 intermolecular adsorption. This effect is attenuated as the number of amino groups present in the organic chain increases. ED (NN) and DT (NNN) molecules, with 2 and 3 amino groups respectively, can undergo intramolecular CO_2 adsorption uptakes. Consequently, the increase of amine loadings lead to smaller increments in their relative adsorption capacity compared to AP (N).

A maximum value of 0.42 is obtained for SBA-15-AP (N)-6 material. Taking into account that 0.5 is the highest value achievable in anhydrous conditions for primary and secondary amines (that is, two amino groups per CO_2

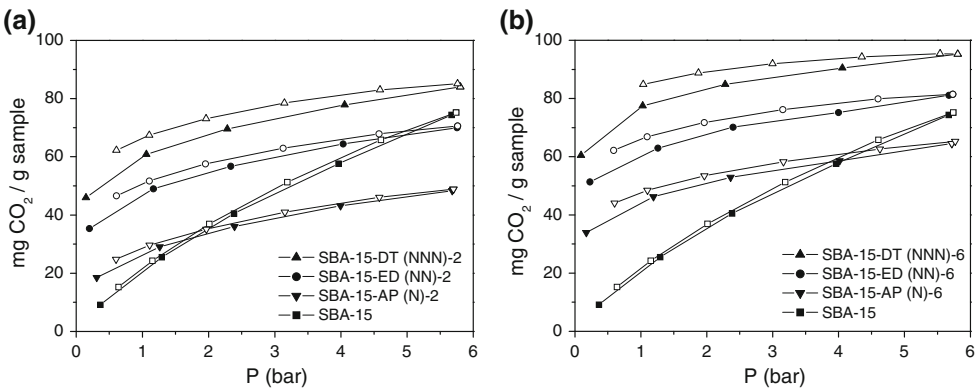

Fig. 4 Pure CO_2 adsorption–desorption isotherms measured at 45 °C for SBA-15 silica and amine-functionalized samples with: (**a**) 2 SiOH/nm^2 and (**b**) 6 SiOH/nm^2

Table 2 Nitrogen content, CO_2 adsorption capacity and relative adsorption capacity per mole of nitrogen of SBA-15 silica and functionalized samples at 45 °C

Adsorbent	wt% N	mg CO_2/g sample		mole CO_2/mole N[a]
		1 bar	5.5 bar	
SBA-15	–	20.3	72.9	–
SBA-15-AP (N)-2	2.6	26.2	48.1	0.32
SBA-15-ED (NN)-2	4.8	46.0	69.6	0.30
SBA-15-DT (NNN)-2	6.3	60.1	83.7	0.30
SBA-15-AP (N)-6	3.7	48.8	67.0	0.42
SBA-15-ED (NN)-6	5.7	60.0	80.8	0.34
SBA-15-DT (NNN)-6	7.3	76.8	94.9	0.34

[a] Data measured at 1 bar

adsorbed molecule to form a carbamate species) [13], it can be deduced that an efficiency of 84 % is achieved at a CO_2 pressure of 1 bar. This value is significantly higher than 52 % obtained in a previous work by our group for equivalent impregnated materials (poly-ethyleneimine (PEI) impregnated SBA-15) [12].

On the other hand, although a small amount of the organic molecules could be allocated within the micropores of the material, it is not clear whether they would significantly contribute to CO_2 adsorption, due to the limited space for diffusion. If these contribution were be negligible, part of the functionalizing molecules would not be efficient for CO_2 adsorption and therefore the efficiency results already mentioned would slightly change.

3.3 Influence of the Drying Step

Functionalized samples SBA-15-AP (N)-6, SBA-15-ED (NN)-6 and SBA-15-DT (NNN)-6 were dried in air atmosphere at 110 °C for different times (6, 24 and 72 h). Textural properties and CO_2 adsorption capacities of samples dried in these conditions were measured and compared with those obtained for the materials dried at room temperature for 24 h.

3.3.1 CO_2 Adsorption

Pure CO_2 adsorption isotherms were carried out at 45 °C for all samples. Table 3 lists CO_2 uptake values at 45 °C and 1 bar and the corresponding nitrogen contents of the samples, obtained by elemental analysis.

The influence of the drying step can be observed on the CO_2 uptake and the organic content variations produced when drying samples at 110 °C. SBA-15 materials functionalized with ED (NN) and DT (NNN) amine molecules show evidence of organic loss when treated at 110 °C in air atmosphere. As seen, nitrogen content has gradually decreased in a small extent for these materials after 72 h. However, AP (N) functionalized materials show no nitrogen loss in the same conditions. Thus, a small fraction of the incorporated organic chain is being lost when materials are dried at 110 °C, but this only happens for those structures that have two or more amino groups in the carbon chain.

However, regarding CO_2 adsorption (Table 3), dried materials at 110 °C show a significant decrease in adsorption capacity, stronger for samples functionalized with ED and DT amine molecules. In the case of SBA-15-ED (NN)-6 and SBA-15-DT (NNN)-6, adsorption capacities after 72 h are 19.5 and 15.2 mg CO_2/g respectively, which are even lower than values obtained for raw SBA-15. Furthermore, molar adsorption capacities per mole of nitrogen (Table 3) also decrease for ED and DT, but not for AP amine molecules. These results are not in agreement

Table 3 Nitrogen content, CO_2 adsorption capacity and relative capacity per mole of nitrogen of SBA-15 and functionalized samples at 45 °C and 1 bar

Adsorbent	Drying temperature (°C)	Drying time (h)	wt% N	mg CO_2/g ads	mol CO_2/mol N
SBA-15	–	–	–	20,3	–
SBA-15-AP (N)-6	20	24	3.7	48.8	0.42
	110	6	3.7	47.7	0.42
	110	24	3.8	49.8	0.42
	110	72	3.7	44.9	0.38
SBA-15-ED (NN)-6	20	24	5.7	60.0	0.34
	110	6	5.6	55.0	0.31
	110	24	5.5	43.7	0.25
	110	72	5.1	19.5	0.12
SBA-15-DT (NNN)-6	20	24	7.3	76.8	0.34
	110	6	7.2	61.9	0.28
	110	24	6.6	32.1	0.15
	110	72	6.3	15.2	0.08

with the small nitrogen loss discussed above. So, the decrease of relative adsorption capacities clearly indicates that besides the partial removal of amino groups during heating at 110 °C, a part of the remaining amino groups probably undergo a chemical reaction, being transformed into different organic groups containing nitrogen species not active for CO_2 adsorption. On the other hand, a pore blocking or a structure damage could also occur during the thermal treatment.

The fact that both adsorption capacity values of AP grafted material (mg CO_2/g and mol CO_2/mol N) are not affected by drying the material at 110 °C indicates that neither loss nor chemical reaction of amino groups occur. This result was also confirmed by elemental analysis measurements (Table 3).

3.3.2 Physicochemical Analysis

In order to evaluate the structure and physical properties of functionalized samples dried in air at 110 °C, X-Ray diffractograms and N_2 adsorption–desorption isotherms were obtained. Figure 5 shows the XRD patterns corresponding to the dried samples AP (N), ED (NN) and DT (NNN). It is observed that no significant variations are found when heating these samples at 110 °C up to 72 h, showing that the SBA-15 porous structure is preserved.

N_2 adsorption–desorption isotherms of dried samples at 110 °C are presented in Fig. 6. As observed, aminopropyl-functionalized sample (AP) as well as sample ED show no variation in N_2 adsorption when drying at 110 °C for 72 h (Fig. 6a, b). However, this is not the case for DT sample, where nitrogen adsorption increases with drying time at 110 °C (Fig. 6c). Therefore, XRD and N_2 adsorption–desorption isotherms of samples dried in air at 110 °C do not explain the loss of CO_2 adsorption capacity with this thermal treatment.

3.3.3 Infrared Spectroscopy Analysis

Infrared spectroscopy was used to check whether a chemical reaction involving amino groups is produced or not when heating functionalized materials in air at 110 °C. Figure 7a shows the FTIR spectrum for ethylene-diamine functionalized sample SBA-15-ED (NN)-6 before thermal treatment, as an example of the resulting spectra for the set of materials. Main absorption peaks have been extensively detailed in the literature [40]. A broad band in the range 3700–3200 cm^{-1} corresponds to O-H stretching from free water and silanol groups (Si-OH). In a similar range, between 3450 and 3300 cm^{-1}, primary and secondary amines also exhibit symmetric and antisymmetric stretching absorption peaks.

At lower wavenumbers two bands can be observed at 2938 and 2889 cm^{-1} and some other minor hidden contributions are probably present behind the previous ones. These absorption bands correspond to antisymmetric and symmetric stretching modes of C–H bonds present in $-CH_2-$, $-CH_2-NH_2$ and $-O-CH_3$ groups, along with the possible overtones due to C-H bending.

Figure 7b shows the most interesting part of the spectrum obtained for ED functionalized sample before thermal treatment. Vibrational bands in the region 1650–1550 cm^{-1} are attributed to bending vibration of N–H in primary and secondary amines. A peak at 1479 cm^{-1} has been assigned to the $-CH_2-$ scissor vibration in an aliphatic chain or anchored to a terminal amino group. Also, in the same range, symmetric and antisymmetric C-H deformations in methoxy groups ($-O-CH_3$) are revealed. Several peaks are detected at lower wavenumbers, between 1385 and 1275 cm^{-1}. Alkane H-C-H and H-N-H deformation vibrations are producing these peaks.

A sharp and intense absorption peak in the range 1200–1000 cm^{-1} is due to siliceous (Si-O-Si) and siloxane

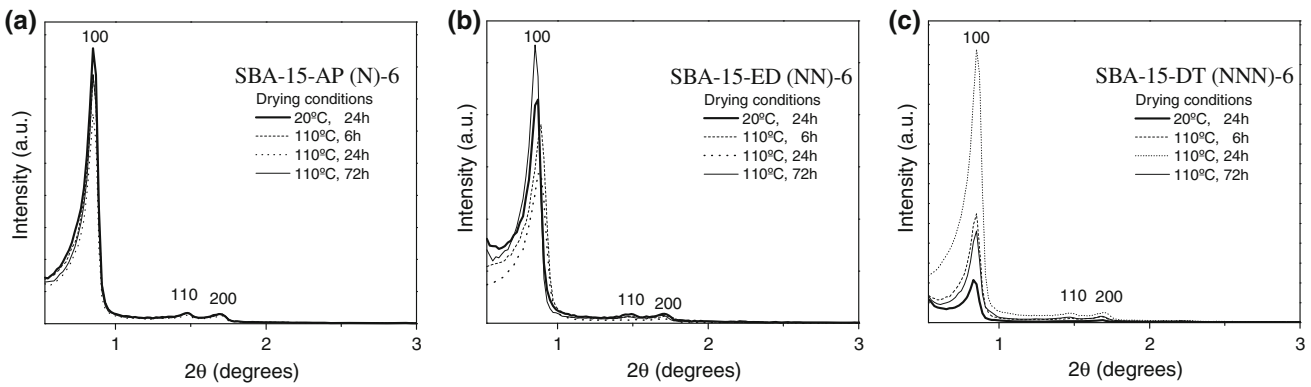

Fig. 5 X Ray Diffractograms obtained for AP (**a**), ED (**b**) and DT (**c**) functionalized samples for different drying conditions: 20 °C for 24 h and 110 °C for 6, 24 and 72 h

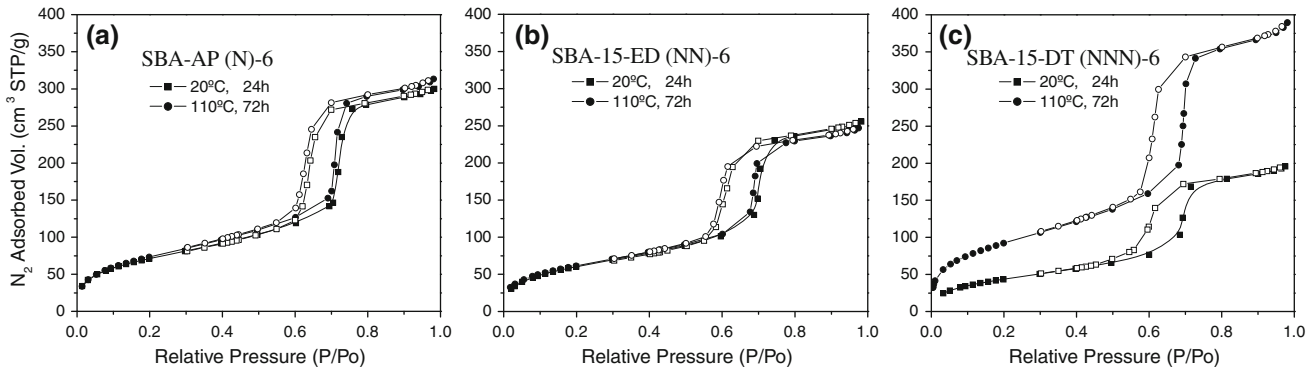

Fig. 6 N_2 adsorption–desorption isotherms for AP (**a**), ED (**b**) and DT (**c**) functionalized samples for different drying conditions: 20 °C for 24 h and 110 °C for 72 h

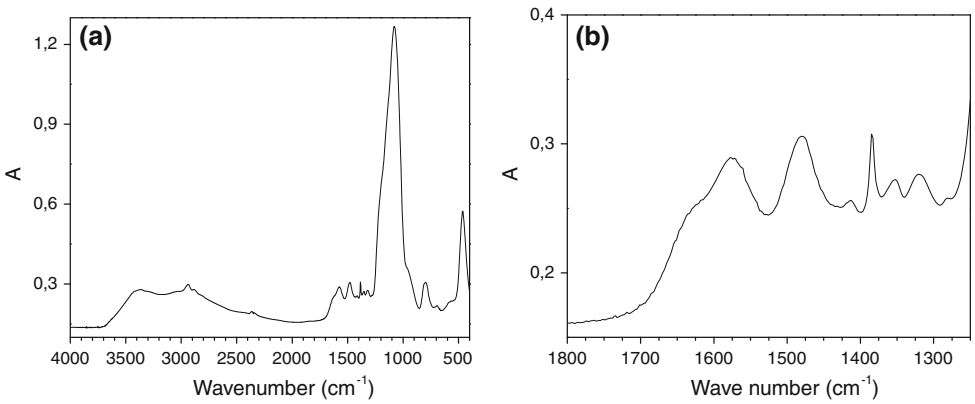

Fig. 7 FTIR spectrum of ethylenediamine (ED) functionalized sample SBA-15-ED (NN)-6 at room temperature

bonds (Si-O-CH_3). The band detected at 800 cm^{-1} can be attributed to C-N primary amine bonds, while the absorption peak appearing at 460 cm^{-1} corresponds to Si-O-C bonds.

Figure 8 shows the results of in situ DRIFTS analysis of the SBA-15-AP (N)-6, SBA-15-ED (NN)-6 and SBA-15-DT (NNN)-6 materials dried in air at 110 °C for several times, up to 85 h (Fig. 8a, b, c) and also under vacuum (Fig. 8d). Analyzing the behaviour of SBA-15-ED (NN)-6 (Fig. 8a), the only significant change observed is that a new band grows progressively at 1667 cm^{-1} as the drying time increases. As it has been previously reported, this absorption band corresponds to the C=N double bond stretching vibration in functional groups such as imine (>C=N-) [41], which is the predominant tautomeric form of enamine (>C=CR_1-N–R_2R_3), oxime (>C=N-OH) [42], nitrone (>C=N^+RO^-…) [43] or more likely, a mixture of all of them, resulting from complex amine oxidation mechanisms. The continuous growing of this band at 1667 cm^{-1} for 85 h points to a slow oxidation mechanism of the amino groups.

Figure 8b shows the infrared spectra for AP-functionalized sample dried at 110 °C under vacuum and then under air atmosphere for various drying times. In this case, the IR spectra exhibit no changes around 1667 cm^{-1}, pointing that there is no oxidation process. This behaviour is in agreement with the CO_2 adsorption capacity and nitrogen content results previously commented, where no changes were produced as a result of drying SBA-15-AP (N)-6 in air at high temperature.

On the contrary, DT-functionalized material does show the appearance of the same band at 1667 cm^{-1} (Fig. 8c), which increases with the drying time, as it happened with the ED-functionalized sample. Besides, this increase of intensity is higher in the case of DT-functionalized sample compared to ED. This can be due to a higher reaction rate of DT molecules or simply to a higher concentration of amino groups in this molecule. These results are also in agreement with the CO_2 adsorption capacity and nitrogen content results previously commented for this material.

A similar thermal treatment at 110 °C was carried out at high vacuum and consequently in the absence of oxygen. The DRIFTS spectra obtained for sample SBA-15-DT (NNN)-6 are plotted in Fig. 8d. As observed, the vibrational spectrum of diethylene-triamine (DT) is not modified, despite of extending the treatment for 85 h. These results clearly show that the atmospheric oxygen is involved in the reaction to accomplish the amine oxidation process.

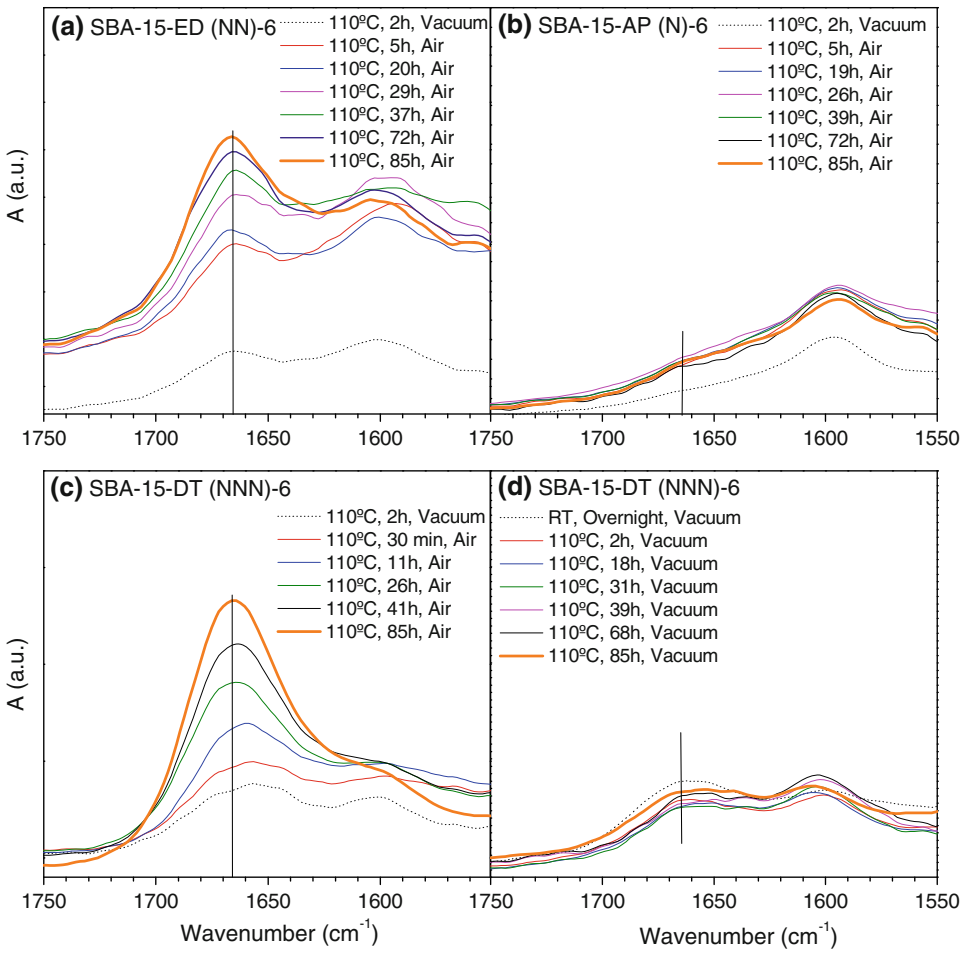

Fig. 8 Study of drying step performed in air at 110 °C up to 85 h for SBA-15-ED (NN)-6 **(a)**, SBA-15-AP (N)-6 **(b)** and SBA-15-DT (NNN)-6 **(c)**. Same study for SBA-15-DT (NNN)-6 under vacuum at 110 °C up to 85 h

The oxidation of amine organosilane molecules was also checked by acquiring the FTIR spectra of raw organosilane precursors heated at 110 °C in air. While spectra of ED and DT resulting samples exhibited a new band at 1667 cm^{-1} once again, AP showed no variation with drying time.

From these results, it can be concluded that the oxidation of amino groups to oxime or imine derivatives lead to the loss of CO_2 adsorption capacity, probably because these groups are not active for carbon dioxide adsorption.

It has to be mentioned that several research works concerning air-oxidation of amines and aminated species for oxime production in the presence of silica have shown the effect of silica as an oxidation catalyst at relative low temperature [44, 45]. Indeed, it has been recently detected that the presence of some silicon defects produced when silica is synthesized via silane hydrolysis could also catalyze some oxidation process [46, 47].

Finally, we discuss the behavior of primary amino groups present in aminopropyl (AP) molecules, compared to ethylenediamine (ED) and diethylenetriamine (DT). It should be recalled that the only difference between AP on the one hand, and ED or DT on the other, is the longer length and the presence of secondary amino groups in ED and DT. It seems that primary amino groups cannot react under mild conditions, or that they cannot accomplish oxidation without having secondary amino groups in its surroundings. According to the literature, secondary amino groups produce intermediate reaction species through an electron donor-acceptor mechanism easier than primary amino groups. Besides, secondary amino groups have shown the best cooperative catalytic efficiency among other amino groups in other reactions [48]. In summary, it seems that although the detailed oxidation mechanism is not clear, secondary amino groups would play a key role on the reaction mechanism.

Previous works testing the stability of grafted materials in air have been based on TGA studies. As an example, aminopropyl (AP) [49] and ethylene-diamine (ED) [50] were heated up to 700 °C at a rate of 10 °C/min in air atmosphere. The results obtained did not show any mass decrease due to a possible organic degradation in the range 200-250 °C, so that the stability of these molecules was claimed.

Our study, which is focused on the effect of drying time at a constant temperature (110 °C), has demonstrated that a significant loss of organic chain does occur and that

chemical changes induced by the combined effect of temperature and time produce a large decrease in CO_2 adsorption capacity.

3.4 Adsorption–Desorption Runs

Several CO_2 adsorption–desorption cycles were carried out at 45 °C for SBA-15-DT (NNN)-6 sample dried at room temperature. After the adsorption step, the desorption step was performed under vacuum (10^{-3} mbar) at 110 °C for 2 h. In these air-free conditions, oxidation reactions of amino groups do not take place, as shown before.

Figure 9 shows the CO_2 adsorption capacity obtained along four consecutive adsorption–desorption cycles. As observed, adsorption capacity measured at 45 °C and 1 bar remains constant, thus proving the material stability. This fact supports the idea that DT functionalized SBA-15 can be considered a promising material to effectively remove CO_2 from fuel combustion gases, which are usually released from power stations at 45 °C and at atmospheric pressure, as commented. However, it must be taken into account that thermal regeneration should be performed in the absence of oxygen.

4 Conclusions

Mesoporous SBA-15 silica materials functionalized with amino groups show suitable adsorption properties for CO_2 capture, being amine-organosilane molecules easily incorporated to SBA-15 materials by grafting techniques. These aminated SBA-15 adsorbents have the advantage over the conventional ethanol-amine based liquid absorption processes that toxicity, corrosion, waste production and mainly energy consumption in material regeneration are significantly lower, being its recovery much easier.

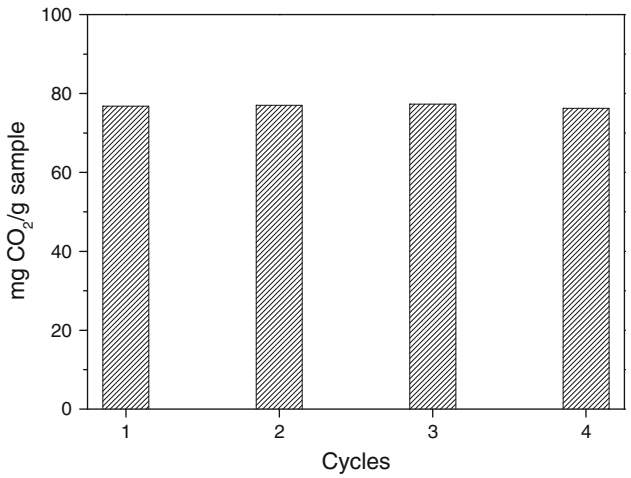

Fig. 9 CO_2 adsorption capacity of SBA-15-DT (NNN)-6 at 45 °C and 1 bar, after several consecutive adsorption–desorption cycles

The drying step of the amine grafted SBA-15 is critical for the CO_2 adsorption properties, since a progressive oxidation of amino groups to oxime and/or imine species can take place when adsorbents containing more than one amino group are dried at 110 °C in the presence of air, thus reducing the adsorption capacity. However, amine functionalized SBA-15 materials dried at room temperature are very efficient for CO_2 adsorption at atmospheric pressure.

The CO_2 adsorption capacity is maintained along the adsorption–desorption cycles, whenever desorption is carried out in non-oxidizing conditions. Vacuum was successfully used for regeneration. However, other lower-cost methods should be developed at industrial scale for material regeneration, provided that no chemical changes are produced in the amino groups.

Acknowledgments This study was carried out within the framework of the CENIT CO2 Project, supported by CDTI—Spanish Industry Department (www.cenitco2.es).

References

1. IPCC (1990) In: Houghton JT, Jenkins GJ, Ephraims JJ (eds) IPCC first assessment report (FAR). IPCC, New York
2. Pachauri RK, Reisinger A (eds) (2007) IPCC Fourth Assessment Report: Climate Change 2007 (AR4). IPCC, Geneva
3. Metz B, Davidson O, de Coninck H, Loos M, Meyer L (eds) (2005) IPCC special report on carbon dioxide capture and storage. IPCC, Cambridge
4. Kyoto Protocol to the United Nations framework convention on Climate Change. United Nations, 1998
5. The economics of adaptation to climate change (2009) World Bank, Bangkok
6. Astarita G (1961) Chem Eng Sci 16:202–207
7. Maddox RN, Mains GJ, Rahman MA (1987) Ind Eng Chem Res 26:27–31
8. Rinker EB, Ashour SS, Sandall OC (2000) Ind Eng Chem Res 39:4346–4356
9. Carbon sequestration. State of Science. (1999) Office of Science and Office of Fossil Energy. US Department of Energy. DOE/OS-FE, Washington DC
10. Tontiwachwuthikul P, Meisen A, Lim CJJ (1991) Chem Eng Data 36:130–133
11. Douglas A, Costas T (2005) Sep Sci Technol 40:321–348
12. Sanz R, Calleja G, Arencibia A, Sanz-Pérez ES (2010) Appl Surf Sci 256:5323–5328
13. Caplow M (1968) J Am Chem Soc 24:6795–6803
14. Oye G, Sjoblom J, Stocker M (2001) Adv Colloid Interface Sci 89:439–466
15. Zhao D, Feng J, Huo Q, Melosh N, Fredrickson GH, Chmelka BF, Stucky GD (1998) Science 279:548–552
16. Xu X, Song C, Andrésen JM, Miller BG, Scaroni AW (2002) Energy Fuel 16:1463–1469
17. Xu X, Song C, Andrésen JM, Miller BG, Scaroni AW (2003) Microporous Mesoporous Mater 62:29–45
18. Xu X, Song C, Miller BG, Scaroni AW (2005) Ind Eng Chem Res 44:8113–8119

19. Wang X, Schwartz V, Clark JC, Ma X, Overbury SH, Xu X, Song C (2009) J Phys Chem C 113:7260–7268
20. Son WJ, Choi JS, Ahn WS (2008) Microporous Mesoporous Mater 113:31–40
21. Chen C, Yang ST, Ahn WS, Ryoo R Chem Commun (2009) 3627–3629
22. Fauth DJ, Filburn TP, Gray ML, Hedges SW, Hoffman JS, Pennline HW, DOE/NETL-IR-2007-156
23. Liu SH, Wu CH, Lee HK, Liu SB (2010) Top Catal 53:210–217
24. Su F, Lu C, Kuo S-C, Zeng W (2010) Energy Fuel 24:1441–1448
25. Bhagiyalakshmi M, Yun LJ, Anuradha R, Jang HT (2010) J Hazard Mater 175:928–938
26. Fisher JC, Tanthana J, Chuang SSC (2009) Environ Prog Sustain Energy 28:589–598
27. Yue MB, Sun LB, Cao Y (2008) Microporous Mesoporous Mater 114:74–81
28. Yue MB, Chun Y, Cao Y (2006) Adv Funct Mater 16:1717–1722
29. Chong ASM, Zhao XS (2003) J Phys Chem B 107:12650–12657
30. Aguado J, Arsuaga JM, Arencibia A, Lindo M, Gascón V (2009) J Hazard Mater 163:213–221
31. Leal O, Bolívar C, Ovalles C, García JJ, Espidel Y (1995) Inorg Chim Acta 240:183–189
32. Huang HY, Yang RT (2003) Ind Eng Chem Res 42:2427–2433
33. Knowles GP, Graham JV, Delaney SW, Chaffee AL (2005) Fuel Process Technol 86:1435–1448
34. Knowles GP, Delaney SW, Chaffee AL (2005) Stud Surf Sci Catal 156:887–896
35. Knowles GP, Delaney SW, Chaffee AL (2006) Ind Eng Chem Res 45:2626–2633
36. Harlick PJE, Sayari A (2007) Ind Eng Chem Res 46:446–458
37. Van der Voort P, Gills-D'Hamers I, Vrancken KC, Vansant EF (1991) Faraday Trans 87:3899–3905
38. Drage TC, Blackman JM, Pevida C, Snape CE (2009) Energy Fuel 23:2790–2796
39. Cavenati S, Grande CA, Rodrigues AE (2004) J Chem Eng Data 19:1095–1101
40. Socrates G (2001) Infrared and Raman characteristic group frequencies. Wiley, UK
41. Ishikawa N, Kitazume T (1972) Chem Lett 169–170
42. Kimura M, Kuroda Y, Yamamoto O, Kubo M (1961) Bull Chem Soc Jpn 34:1081–1086
43. Lebel NA, Banucci E (1971) J Org Chem 36:2440–2448
44. Armor JN (1982) U.S. Patent 4.337.358
45. Armor JN, Zambri PM (1982) J Catal 73:57–65
46. Matsumura Y, Hashimoto K, Moffat JB (1992) J Phys Chem 96:10448–10449
47. Trejda M, Ziolek M, Decyk P, Duczmal D (2009) Microporous Mesoporous Mater 120:214–220
48. Xie Y, Sharma KK, Anan A, Wang G, Biradar AV, Asefa T (2009) J Catal 265:131–140
49. Khatri RA, Chuang SSC, Soong Y, Gray M (2006) Energy Fuel 20:1514–1520
50. Wei J, Shi J, Pan H, Su Q, Zhu J, Shi Y (2009) Microporous Mesoporous Mater 117:596–602